# *Original Research Article*

**Electroconductivity of steady viscous MHD incompressible fluid between two porous parallel plates provoked by chemical reaction and radiation**

**Abstracts**

The effect of electroconductivity on MHD fluid flow through an even pore spaces on two parallel plates was carried out. Solution to the governing equations and analysis of the resulting parameters showedthat an increase in Schmidt number and Chemical reaction result in an increase in both the concentration and velocity profiles of the fluid. The increase in Prandtl number and radiation parameter also led to a decrease in the temperature and velocity profiles of the fluid. An increase in Reynolds number, Grashof number due to temperature and concentration all led to an increase in velocity profile of the fluid while Hartmann number and Electroconductivity bring about a decrease in the velocity profile of the fluid. Special cases of the fluid configuration, Shear stress, Nusselt number and Sherwood number was also examined.

**Keywords**: Porous parallel plates, MHD, Viscous Incompressible Fluid, Couette flow, Poiseuille flow, Electoconductivity

PACS: 47.10.Fg

## 1. Introduction

Porous plates or surfaces are even or uneven holes that are found on plates or substancesfor fluids and other finely elements to flow through. The rate of flow depends on so many factors ranging from nature of pores, grain size or shape, sorting, clay and organic content to mention few. They are created as a result of anthropogenic activities intentional or unintentional and some clay particles which tend to electrostatically repel one another along the surface of the particles and create void spaces. In plasma dynamics such as the depletion of the ozone layer [1] and decrease of

granules by pressure dependent forces on isothermal and adiabatic fluids [2] are widely studied. The formulation and application of Darcy's law is also depended on fluid through porous medium though for slow flow and small Reynolds number characteristics. The study of flow through porous plates or surfaces has been widely studied in recent times due to its applications in geothermal and oil recovery process, movement of fluid in xylem and phloem vessels in plants , perspirations through pore spaces in humans, and tunneling. Others are Josephson junction,

and construction of buildings. The viscosity and pressure of such flow has also been vigorously studied and its results documented. Orukari et al [3], studied the motion of fluid through porous medium and made useful findings. Anand et al [4] in their investigation of fluid flow in a porous medium with other parameters, opined that its effect have both physical and engineering value which must be investigated properly. Studies of the effect of MHD, porosity and radiation in conjunction with other parameters are also abounded [5-15] and their contributions are not only vital but far reaching. Recently, Ullah et al [16] considered squeezing flow in porous medium with MHD effect and showed using graphs that both imposed magnetic field and constant electroconductivity are directly proportional to the velocity field. The interplay of a combination of two or more of these parameters in this flow configuration has attracted researchers to it. Studies of the special cases in which the flow result into Couette flow and Poiseuille flow [17 and 18], is also very common with a combination of parameters. Therefore, our aim is to critically examine the effect of magnetic field and electroconductivity to the flow configuration and compare with existing results which we hope will add to the body of literatures.

**Nomenclature**

| | |
|---|---|
| $\rho$ = Fluid density | $u'$ = fluid velocity |
| P= fluid pressure | U = plate velocity |
| $\sigma_\infty$ = constant fluid electroconductivity | $\mu$ = absolute viscosity |
| $\sigma_0$ = dimensionless fluid electroconductivity | $B_0^2$ = Magnetic field |
| $\sigma$ = fluid conductivity | Re = Reynolds number |
| u = dimensionless fluid velocity | H = Magnetic Hartmann number |

| | |
|---|---|
| $p'$ = dimensionless fluid pressure | x,y = coordinates |
| $\eta$ = dimensionless coordinate | D= Chemical molecular diffusivity |
| a = thermal diffusivity | $\beta_T$ = coefficient of volume expansion for temperature |
| $C'$ = fluid concentration | $\beta_c$ = coefficient of volume expansion for concentration |
| $C_o$ = characteristic concentration | T = fluid temperature |
| $T_o$ = characteristic temperature | $K_r^2$ = chemical reaction term |
| $Gr_T$ = free convection parameter due to temperature | $q_y$ = radiative term |
| $Gr_c$ = free convection parameter due to concentration | $\theta$ = dimensionless temperature |
| $\sigma_0$ = dimensionless fluid electroconductivity | $C_p$ = specific heat at constant pressure |
| $\wedge$ = Planck's function | $\alpha_{K^*}$ = absorption coefficient |
| $\kappa^*$ = frequency of radiation | $\sigma_c$ = Stefan Boltzmann constant |
| $R$ = dimensionless radiation term | $k$ = dimensionless chemical reaction term |
| Sc = Schmidt number | Pr= Prandtl number |

## 2. Mathematical Model Formulation

We consider steady laminar flow of viscous incompressible fluid between two infinite parallel porous plates separated by a distance 2h as shown in figure 1.

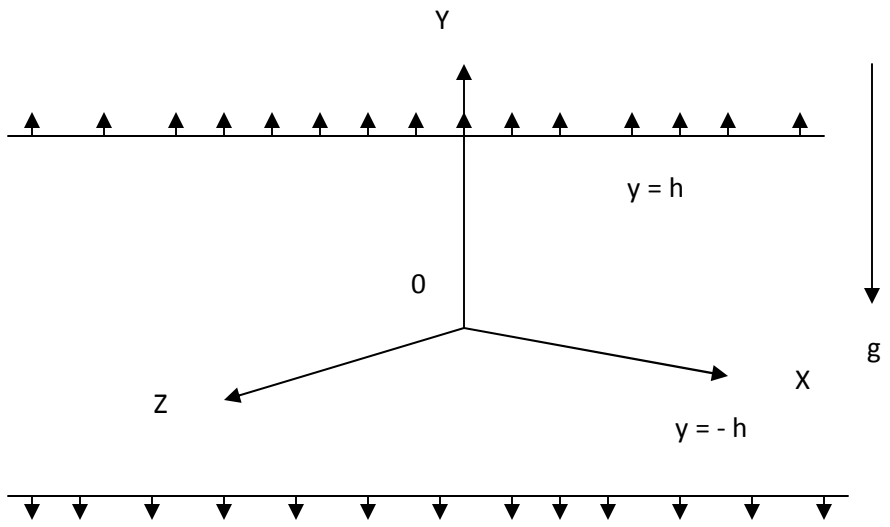


Figure 1: Physical model and coordinate system of the problem

Let $x$ be the direction of the main flow, $y$ be the direction perpendicular to the flow and the width of the plates parallel to the $z-$direction. We also assume the velocity component w to be zero everywhere and the velocity u as a function of $y$ alone. The continuity equation reduces to

$$\frac{\partial u'}{\partial y} = 0 \qquad (1)$$

so that v does not vary with $y$ .

The assertion implies that, the fluid enters the flow region through the lower plate at constant velocity $v_0$ and leaves through the upper plate.

The geometry of the fluid reduces the Navier-Stokes equations into the form

$$v_0 \frac{\partial u'}{\partial y} = -\frac{1}{\rho}\frac{\partial p}{\partial x} + \mu \frac{\partial^2 u'}{\partial y^2} - \frac{\sigma B_0^2 u'}{\rho} - \frac{\sigma_\infty u'}{U} + g\beta_T (T - T_0) + g\beta_C (C - C_0) \qquad (2)$$

$$0 = -\frac{1}{\rho}\frac{\partial p}{\partial y} \qquad (3)$$

where following Boricic et al [19], the fluid electroconductivity is assumed to be of the form $\sigma_\infty \left(1 - \frac{u'}{U}\right)$ but for physical exigency and mathematical amenability, it is approximated to the form in equation (2). Using the no-slip condition, the boundary conditions are

$$u(-h) = 0, \quad u(h) = U \tag{4}$$

From equation (2), differentiate with respect to x, simplify and integrate with respect to x, we get

$$\frac{\partial p}{\partial x} = -p \tag{5}$$

where the negative sign introduced, describe a decrease in p as x increases.

If we put equation (5) into equation (2) and simplify, we get

$$\frac{\partial^2 u'}{\partial y^2} - \frac{v_0}{\mu}\frac{\partial u'}{\partial y} - \frac{\sigma B_0^2 u'}{\mu\rho} - \frac{\sigma_\infty u'}{\mu\rho} + \frac{g\beta_T (T - T_0)}{\mu\rho} + \frac{g\beta_C (C - C_0)}{\mu\rho} = -\frac{p'}{\mu\rho} \tag{6}$$

$$v_0 \frac{\partial T}{\partial y} = a\frac{\partial^2 T}{\partial y^2} - \frac{1}{\rho C_p}\frac{\partial q_y}{\partial y} \tag{7}$$

$$v_0 \frac{\partial C'}{\partial y} = D\frac{\partial^2 C'}{\partial y^2} - \frac{1}{\rho C_p} k_r^2 C' \tag{8}$$

$$\frac{\partial^2 q_y}{\partial y^2} - 3\sigma_c{}^2 q_y - 16\sigma_c T_\infty^3 \frac{\partial T}{\partial y} = 0 \tag{9}$$

For optically thin medium with relatively low density in the spirit of Cogley et al [20], equation (9) reduces to

$$\frac{\partial q_y}{\partial y} = 4\delta^2 (T - T_0) \tag{10}$$

where $\delta^2 = \int_0^\infty (\alpha_{K^*} \frac{\partial \wedge}{\partial T}) dk^*$

### 2.1 Dimensionless analysis

For dimensional homogeneity of the hydrodynamic equations, we substitute the following dimensionless numbers and parameters

$$\mathrm{Re}=\frac{v_0 h}{\mu}, H=\frac{\sigma B_0^2 v_0 y}{\mu\rho U^2}, \sigma_0=\frac{\sigma_\infty v_0 x}{\mu\rho\sigma u^2}, p'=\frac{p v_0 y}{\rho\mu U^2}, \eta=\frac{y}{h}, u=\frac{u'}{U}, \mathrm{Pr}=\frac{v_0}{a}$$

$$Sc=\frac{v_0}{D}, \theta=\frac{(T-T_0)}{T_\infty}, C=\frac{(C'-C_0)}{C_\infty}, Gr=\frac{g\beta_T(T'-T_0)h^3}{v_0^3}, Gc=\frac{g\beta_T(C'-C_0)h^3}{v_0^3}$$

$$R=\frac{4\delta^2\rho_\infty C_\infty y^2}{\rho C_p \mu}, k=\frac{k_r^2 T_\infty v_0}{\sigma u^3}$$

having employed the Buckingham-- $\pi-$Theorem, equations (6-8) can be rewritten as

$$\frac{\partial^2 u}{\partial\eta^2}-\mathrm{Re}\frac{\partial u}{\partial\eta}-(H+\sigma_0)u+Gr\theta+GcC=-p' \qquad (11)$$

$$\frac{\partial^2\theta}{\partial\eta^2}-\mathrm{Pr}\frac{\partial\theta}{\partial\eta}-R\theta=0 \qquad (12)$$

$$\frac{\partial^2 C}{\partial\eta^2}-Sc\frac{\partial C}{\partial\eta}-kC=0 \qquad (13)$$

with the boundary conditions

$$u(-1)=0, u(1)=U,\ \theta(-1)=0, \theta(1)=\theta_y,\ \ C(-1)=0, C(1)=C_y \qquad (14)$$

**3 Method of Solution**

The solution of equation (13) after the imposition of the appropriate boundary conditions of equation (14) is

$$C=a_{11}\exp\alpha_1\eta+a_{12}\exp\alpha_2\eta \qquad (15)$$

where $a_{11}=\dfrac{C_y\exp-\alpha_2}{\exp-\alpha_2(\exp\alpha_2-\exp-\alpha_2\exp 2\alpha_1)}$

$$a_{12}=\frac{C_y}{\exp\alpha_2-\exp-\alpha_2\exp 2\alpha_1}$$

$$\alpha_{1,2}=\frac{Sc\pm\sqrt{Sc^2+4k}}{2}$$

Considering equation (12), the solution following the same method employed in equation (13), is

$$\theta = b_{11}\exp\alpha_3\eta + b_{12}\exp\alpha_4\eta \tag{16}$$

where $b_{11} = \dfrac{\theta_y \exp-\alpha_4}{\exp-\alpha_4\left(\exp\alpha_4 - \exp-\alpha_4 \exp 2\alpha_3\right)}$

$$b_{12} = \frac{\theta_y}{\exp\alpha_4 - \exp-\alpha_4 \exp 2\alpha_3}\ ,\quad \alpha_{3,4} = \frac{\mathrm{Pr}\pm\sqrt{\mathrm{Pr}^2+4R}}{2}$$

Also, using the same method, the solution of equation (11) is,

$$u = C_{11}\exp\alpha_5\eta + C_{12}\exp\alpha_6\eta + A\exp\alpha_3\eta + B\exp\alpha_4\eta + C\exp\alpha_1\eta + D\exp\alpha_2\eta + E \tag{17}$$

where $A = \dfrac{-Grb_{11}}{\alpha_3^2 - \mathrm{Re}\alpha_3 - (H+\sigma_0)}, \qquad B = \dfrac{-Grb_{12}}{\alpha_4^2 - \mathrm{Re}\,\alpha_4 - (H+\sigma_0)}$

$$C = \frac{-Gca_{11}}{\alpha_1^2 - \mathrm{Re}\alpha_1 - (H+\sigma_0)}\ ,\quad D = \frac{-Gca_{12}}{\alpha_2^2 - \mathrm{Re}\alpha_2 - (H+\sigma_0)}$$

$$E = \frac{p'}{(H+\sigma_0)},\ C_{11} = \frac{-\varphi_{11}\exp\alpha_6 - U\exp-\alpha_6 + \varphi_{12}\exp-\alpha_6}{\exp\alpha_6\exp-\alpha_5 - \exp-\alpha_6}$$

$$C_{12} = \frac{U - \varphi_{12} + \varphi_{11}\exp\alpha_5}{\exp\alpha_6 - \exp\alpha_5\exp\alpha_6}\ ,\quad \alpha_{5,6} = \frac{\mathrm{Re}\pm\sqrt{\mathrm{Re}^2+4(H+\sigma_0)}}{2}$$

$$\varphi_{11} = A\exp-\alpha_3 + B\exp-\alpha_4 + C\exp-\alpha_1 + D\exp-\alpha_2 + E$$

$$\varphi_{12} = A\exp\alpha_3 + B\exp\alpha_4 + C\exp\alpha_1 + D\exp\alpha_2 + E$$

### 3.1 Shear stress

$$\sigma_{xy} = \mu\frac{du}{d\eta} = \mu(C_{11}\alpha_5\exp\alpha_5\eta + C_{12}\alpha_6\exp\alpha_6\eta + A\alpha_3\exp\alpha_3\eta + B\alpha_4\exp\alpha_4\eta + C\alpha_1\exp\alpha_1\eta + D\alpha_2\exp\alpha_2\eta \tag{18}$$

This reveals that the shear stress at the wall of the plates is independent of the pressure gradient.

### 3.2 Skin friction

The skin frictions at the plates $\eta = -1$ and $\eta = 1$ from equation (18) are given as

$$\left[\sigma_{xy}\right]_{\eta=-1} \tag{19}$$

$$\left[\sigma_{xy}\right]_{\eta=1} \tag{20}$$

### 3. 3 Coefficient of friction

The mean fluid flow velocity for our study referring to Rasinghania [17] is

$$u_a = \int_{-1}^{1} u d\eta \tag{21}$$

The coefficient of friction $(C_f)$ corresponding to $\left[\sigma_{xy}\right]_{\eta} = -1$ is $C_f^{-1} = \frac{[\sigma xy]_{\eta=-1}}{0.5\rho u_a^2}$

Similarly, $(C_f)$ corresponding to $\left[\sigma_{xy}\right]_{\eta} = 1$ is $C_f^{1} = \frac{[\sigma xy]_{\eta=1}}{0.5\rho u_a^2}$

The mean $\frac{1}{2}\left(C_f^{-1} + C_f^{1}\right)$ is extensively used in determining the energy losses in the porous channels through which the fluid flows.

### 3.4 Nusselt number

The Nusselt number (Nu) which is the dimensionless heat transfer coefficient is given by

$$Nu = -\left(\frac{d\theta}{d\eta}\right) = -\left(b_{11}\alpha_3 \exp\alpha_3\eta + b_{12}\alpha_4 \exp\alpha_4\eta\right) \tag{22}$$

At the wall of the plates, Nu is given by

$$\left[\frac{d\theta}{d\eta}\right]_{\eta=\pm 1} \tag{23}$$

### 3.5 Sherwood number

The dimensionless mass transfer coefficient (Sh) of the fluid flow is given by

$$Sh = -\left(\frac{dC}{d\eta}\right) = -(a_{11}\alpha_1 \exp\alpha_1\eta + a_{12}\alpha_2 \exp\alpha_2\eta) \tag{24}$$

At the plates, we have

$$\left[\frac{dC}{d\eta}\right]_{\eta=\pm 1} \qquad (25)$$

Emperically, the rate of mass transfer coefficient is related to the Reynolds' number and Schmidt number

$Sh = \xi\sqrt{\mathrm{Re}\ Sc}$ where $\xi$ is a constant (26)

It is therefore important to note that the transition from laminar flow to turbulence flow can also be determined by equation (26)

### 3.6 Special cases

**Case 1.** Plane Couette flow

In this flow configuration, what drives the flow is the relative movement of the plates. Therefore, the pressure gradient is absent and reduces equation (17) to

$$u = C_{11}\exp\alpha_5\eta + C_{12}\exp\alpha_6\eta + A\exp\alpha_3\eta + B\exp\alpha_4\eta + C\exp\alpha_1\eta + D\exp\alpha_2\eta \quad (27)$$

This affected the magnitude of the fluid velocity and by extension the shear stress and the skin friction.

**Case 2**: Plane Poiseuille flow

The configuration for plane Poiseuille flow shows that the plates are at rest because what drives the motion is the pressure gradient. Therefore, U = 0 and the affected parameters in equation (17) are $C_{11}$ and $C_{12}$ which also affected the flow velocity, shear stress and skin friction.

### 4.0 Results and discussion

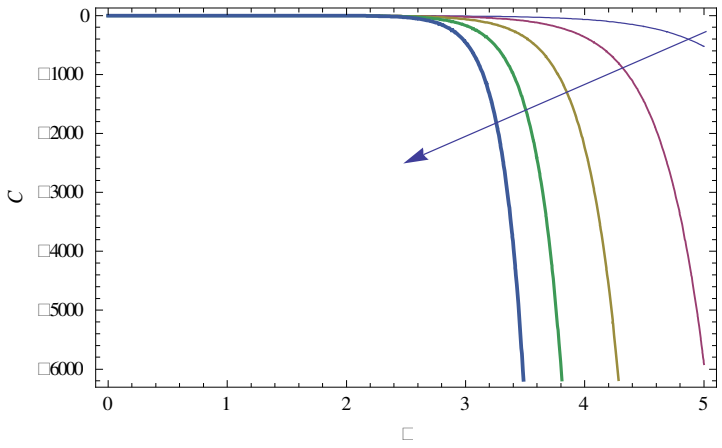

**Figure 2**: Concentration profile $C$ against boundary layer $\eta$ for varying `Schmidt number` $Sc$

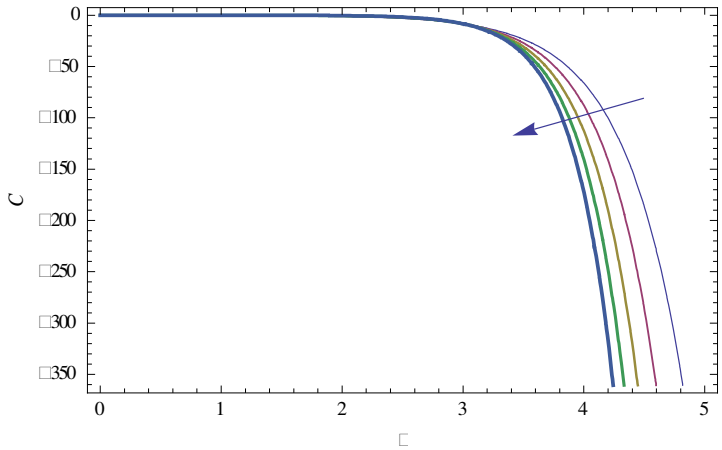


**Figure 3**: Concentration profile $C$ against boundary layer $\eta$ for varying `chemical reaction` $k$

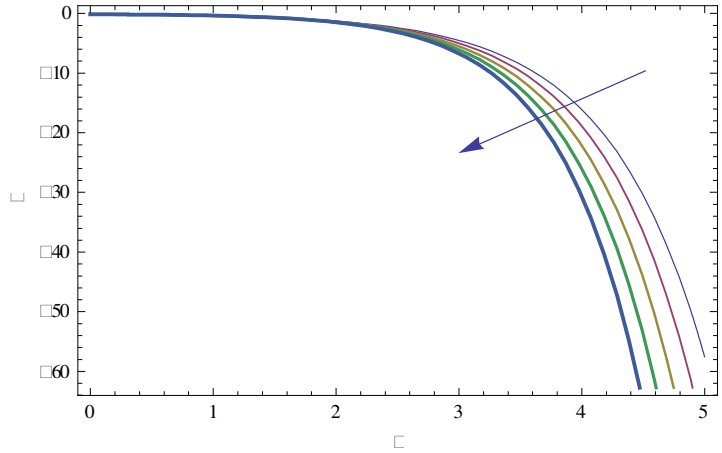


**Figure 4**: Temperature profile $\theta$ against boundary layer $\eta$ for varying `prandtl number` Pr

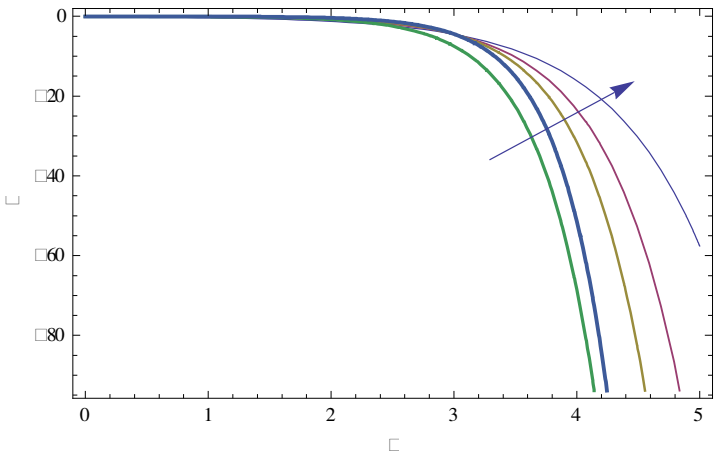


**Figure 5**: Temperature profile $\theta$ against boundary layer $\eta$ for varying `Radiation parameter R`

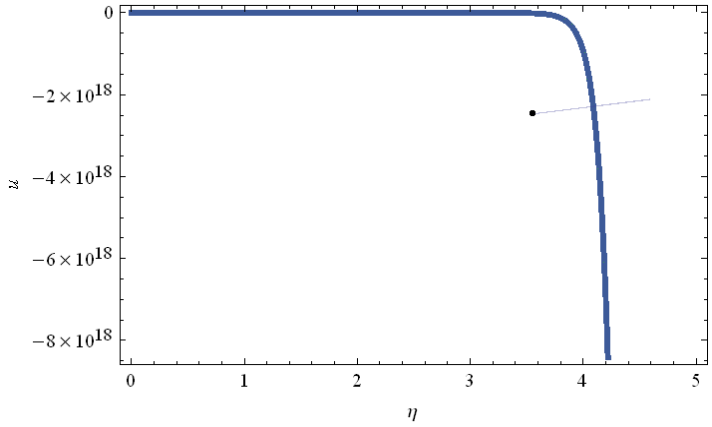


**Figure 6**: Velocity profile $u$ against boundary layer $\eta$ for varying Grashof number $Gr$

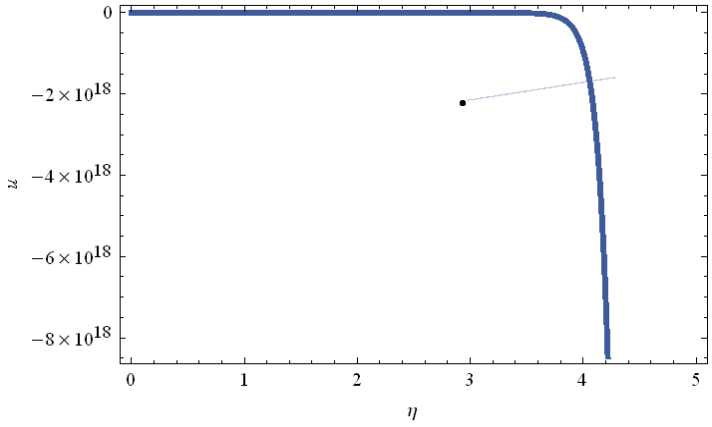


**Figure 7**: Velocity profile $u$ against boundary layer $\eta$ for varying Grashof number $Gc$

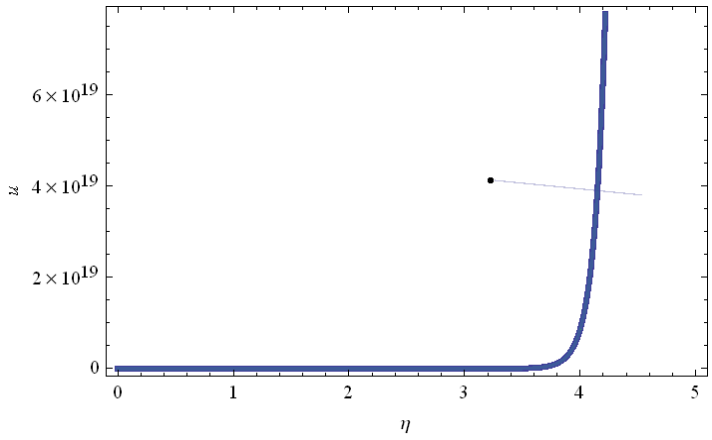


**Figure 8**: Velocity profile $u$ against boundary layer $\eta$ for varying `Schmidt number` $Sc$

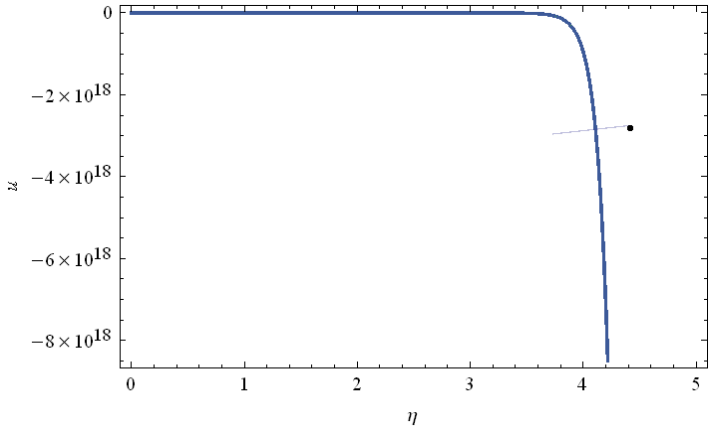


**Figure 9**: Velocity profile $u$ against boundary layer $\eta$ for varying `chemical reaction` $k$

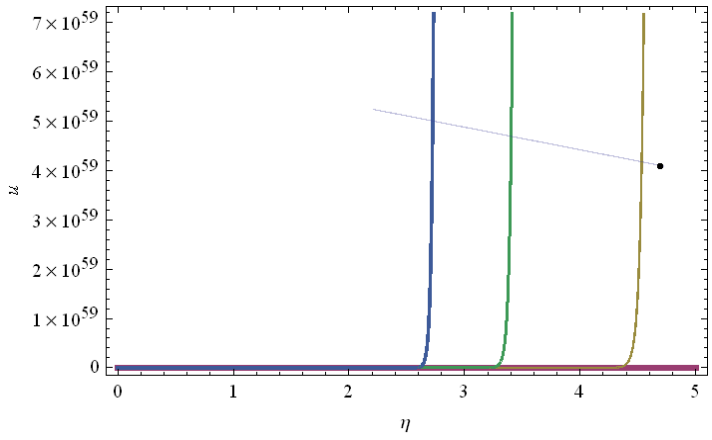


**Figure 10**: Velocity profile $u$ against boundary layer $\eta$ for varying `Reynolds number Re`

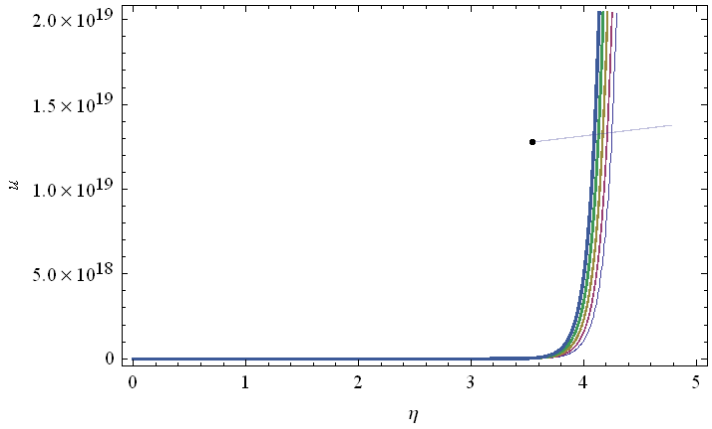


**Figure 11**: Velocity profile $u$ against boundary layer $\eta$ for varying `Hartmann number H`

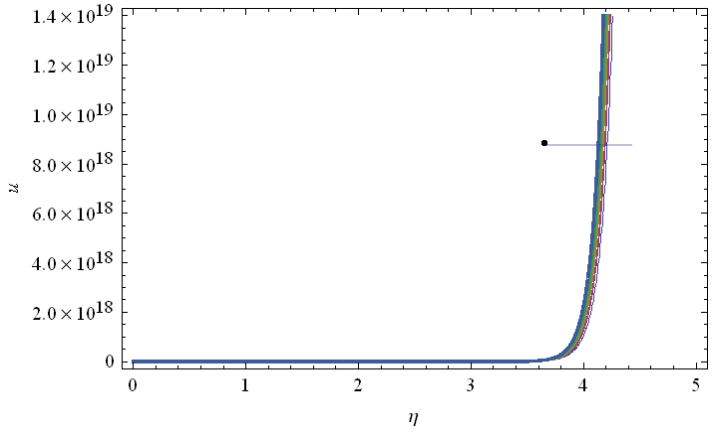


**Figure 12**: Velocity profile $u$ against boundary layer $\eta$ for varying `Electrconductivity` $\sigma_0$

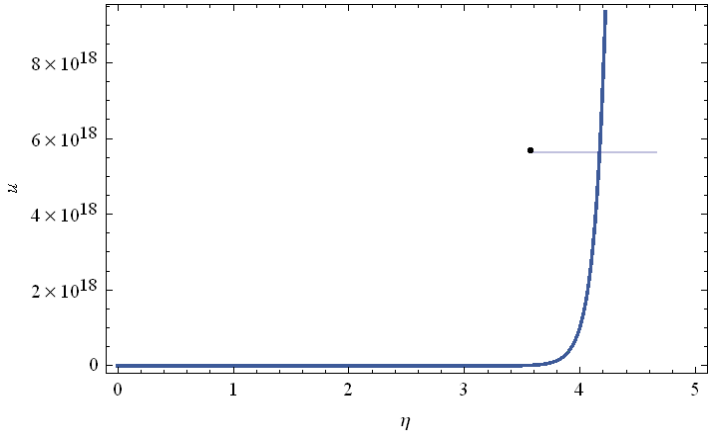


**Figure 13**: Velocity profile $u$ against boundary layer $\eta$ for varying `Prandtl number` Pr

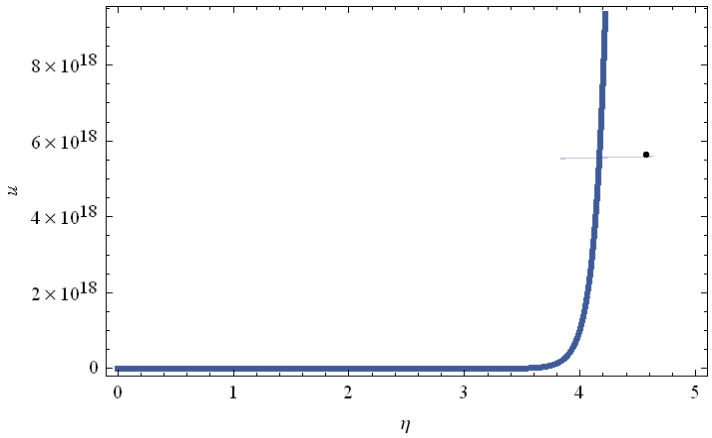


**Figure 14**: Velocity profile $u$ against boundary layer $\eta$ for varying `Radiation parameter R`

In order to get physical insight and numerical validation of the problem, an approximate values of

$P' = 5, U = \theta_y = C_y = 3.26$ are chosen. The values of other parameters made use of are

$\mathrm{Re} = 10,0,20.0,30.0.40.0,50.0$
$Gr = 0.8,1.6,2.4,3.2,4.0$
$H = 0.5,1.5,2.5,3.5,4.5$
$\sigma_0 = 0.25,0.75,1.25,1.75,2.25$
$\mathrm{Pr} = 0.31,0.41,0.51,0.61,0.71$
$R = 1.23,2.23,3.23,4.23,5.23$
$Gc = 0.7,1.4,2.1,2.8,3.5$
$Sc = 0.94,1.94,2.94.3.94,4.94$
$k = 2.34,3.34,4.34,5.34,6.34$

The Schmidt number relates the relative thickness of the hydrodynamic boundary layer and mass boundary layer. It is a ratio of momentum diffusivity to mass diffusivity. Its increase as depicted on Figures (2) and (8) showed a reduction in the boundary layers hence a decrease in the concentration and velocity profiles of the fluid. The chemical reaction of the fluid, reduced the concentration boundary layers but unaffected by the momentum boundary layers. As a result of increase in chemical reaction parameter as shown on Figures (3) and (9), the velocity and concentration profiles of the fluid are reduced considerably. Increase in the prandtl number decrease the thermal boundary thickness and also lower the mean temperature within the boundary layer. Therefore, increase in Prandtl number as shown in Figures (4) and (13) respectively led to a decrease in the temperature and velocity profiles of the fluid. Figures (5) and (14) showed increase in radiation parameter. Radiation which is brought about by thermal transfer, decrease both the temperature and velocity profiles of the fluid flow. Reynolds number examine the transition of fluid from laminar to turbulence from Reynolds number 0 to about 3000. Figure (10) is clear that increase in Reynolds number shows a corresponding increase in the

velocity profile of the fluid. The Hartmann number and electroconductivity are resistive type of forces which tend to impede the flow of fluid in a region where its effect is prevalent. As shown in Figures (11) and (12) respectively, their increase, decrease or reduce the motion or velocity of the fluid flow. The Grashof number due to temperature which is the free convection effects correspond to cooling of the plate $(Gr > 0)$ by natural convection. Its effect, conduct heat away from the plates into the fluid thereby increasing the temperature of the fluid which in turn increases the velocity of the fluid as shown in Figure (6). A similar observation is also reported by an increase in the Grashof number due to concentration (Gc) as depicted in Figure (7). As the Grashof number due to concentration $(Gc > 0)$ increases, the ratio of the buoyancy force to the viscous hydrodynamic force increases, hence result in an increase in the velocity profile of the fluid. From equation (18), the shear stress at the wall of the plates only depicts an increase in magnitude of the fluid velocity considering the no-slip condition adopted. Increase in the material parameters considered will certainly result in the opposite of the heat transfer coefficient as shown in equation (22). Similar observation is also prevalent in the mass transfer coefficient as shown In equation (24). These observations are consistent with the works of [21] and [22].

## 5.0 Conclusions

In this paper, the plates pore spaces are evenly spread and the flow considered, therefore the inclusion of the effect of porosity is ignored. The choice of the boundary conditions and the flow configuration, created two special cases which was discussed by the determination of the shearing stress and skin friction in both cases.

## References

[1] Ngiangia, A.T; Amadi, O and Orukari, M.A (2011). The Effect of Radiation and Chemical Reaction on the Depletion of the Ozone Layer. *Continental Journal of Renewable Energy, 2(1),* 19-25

[2] Ngiangia, A.T and Orukari M.A (2014 ). An Unsteady MHD Flow Past a Porous Medium with Oscillatory Suction Velocity and Newtonian Heating. *International Journal of Materials Physics. 5(1), 27-34*

[3] Orukari, M.A; Ngiangia, A.T & Life-George, F (2011). Influence of Viscous Dissipation and Radiation on MHD Couette Flow in a porous Medium. *Journal of the Nigerian Association of Mathematical Physics, 18,* 201-208

[4] J. Anand Rao, R.Srinivasa Raju, S. Sivaiah, (2012) . Finite element solution of heat and mass transfer in MHD flow of a viscous fluid past a vertical plate under oscillatory suction velocity, J. App. Fluid Mech. 5(3) 1–10

[5] Ngiangia, A.T and Wonu, N (2007). The effect of permeability and radiation on the stability of Couette Flow in a porous Medium: *Journal of Applied Sciences and Environmental Management (JASEM)*, 11(2), 209-214

[6] Ngiangia, A.T (2007). The Effect of Permeability and Radiation on the Stability of Plane Couette-Poiseuille flow in a porous Medium. *Journal of the Nigerian Association of Mathematical Physics, 11, 87-94.*

[7] P Mebine. (2007) Radiation effect on MHD Couette flow with heat transfer between two parallel plates. Global Journal of Pure and Applied Mathematics. **3(2)** 191-202

[8] Ngiangia, A.T and Orukari M.A (2014 ). An Unsteady MHD Flow Past a Porous Medium with Oscillatory Suction Velocity and Newtonian Heating. *International Journal of Materials Physics. 5(1), 27-34*

[9] Ngiangia, A.T; Ojekudo, N; Amadi, O & Orukari, M.A (2011). Onset of instability of MHD Coutte-Poiseuille Flow in a Porous Medium. *Journal of the Mathematical Association of Nigeria (ABACUS), 38(2), 1-16*

[10] Ngiangia, A.T and Orukari M.A (2013 ). MHD Couette-Poiseuille Flow in a Porous Medium. *Global Journal of Pure and Applied Mathematics. 9(2).*169-181

[11]B.PrabhakarReddy.(2015)MHD flow over a vertical moving porous plate with viscous dissipation by considering double diffusive convection in the presence of chemical reaction, Int. J. Adv. Math. and. Mech. 2(4) 73–83

[12] A. J. Bala, S.V.K. Varma, Unsteady MHD heat and mass transfer flow past a semi infinite vertical porous moving plate with variable suction in the presence of heat generation and homogeneous chemical lreaction, Int.J.ofAppl. Math. And Mech. 7(7) (2011) 20 – 44

[13] M. S. Alam. (2014) Unsteady MHD free convective heat transfer flow along a vertical porous flat plate with internal heat generation, Int. J. Adv. Math. and. Mech. 2(2) 52–61

[14] V. Rajesh, S.V.K. Varma. (2009) . Radiation and mass transfer effects on MHD free convection flow past an exponentially accelerated vertical plate with variable temperature. ARPN J. of Eng. and Appl. Sci. 4(6) 20 – 26

[15] A. Postelnicu. (2007) . Influence of chemical reaction on heat and mass transfer by natural convection from vertical sur- faces in porous media considering Soret and Dufour effects, Heat Mass Tranf. 43 595–602

[16] U Inayat, M T llah, R Rahim, K Hamid and Q Mubashir. (2016) Analytical analysis of squeezing flow in porous medium with mhd effect U.P.B. Sci. Bull., Series A, **78(2)** 281-292

[17] M D Raisinghania. (2003). Fluid Dynamics with Hydrodynamics(New Delhi: S. Chand and Company) p 661

[18] J Spurk. (1997). Fluid Mechanics. (New York: Springer) p 178

[19] Z Boricic, D Nikodijevic, D Milenkovic, and Z Stamenkovic. (2005). A form of MH D universal equation of unsteady incompressible fluid flow with variable electroconductivity on heated moving plate Theor. and Appl. Mech, **32(1)** 65-77

[20] A.C. Cogley, W.G. Vincent and S.E. Giles. (1968). Differential approximation to radiative heat transfer in a non-grey gas near equilibrium, The American Inst. Aeronautics and Astronautics. 6 551–553

[21] G Aruna, S V Varma and R S Raju. (2015). Combined influence of Soret and Dufour effects on unsteady hydromagnetic mixed convective flow in an accelerated vertical wavy plate through a porous medium. International Journal of Advances in Applied Mathematics and Mechanics **3(1)** 122-134

[22] K. Sudhakar, R.SrinivasaRaju and M.Rangamma. (2013) Hall Effect on unsteady MHD flow past along a porous flat plate with thermal-diffusion, diffusion-thermo and chemical reaction. International Journal of Physics. and Mathematics. Science. 4(1) 370–395